HHS Public Access

Author manuscript

J Immunol. Author manuscript; available in PMC 2024 September 15.

Published in final edited form as:

J Immunol. 2024 March 15; 212(6): 962–973. doi:10.4049/jimmunol.2300671.

Beta actin G342D as a cause of natural killer cell deficiency impairing lytic synapse termination

Abigail E. Reed[*], **Jackeline Peraza**[‡], **Frederique van den Haak**[*], **Evelyn R. Hernandez**[†], **Richard A. Gibbs**[§], **Ivan K. Chinn**[¶], **James R. Lupski**[‖], **Enrica Marchi**[#], **Ran Reshef**[**], **Bachir Alobeid**[††], **Emily M. Mace**[†], **Jordan S. Orange**[*]

[*]Department of Pediatrics; Department of Microbiology and Immunology, Columbia University Irving Medical Center, New York, NY, USA.

[‡]Department of Biology, Barnard College of Columbia University, New York, NY, USA.

[†]Department of Pediatrics, Columbia University Irving Medical Center, New York, NY, USA.

[§]Department of Molecular and Human Genetics; Human Genome Sequencing Center, Baylor College of Medicine, Houston, TX, USA.

[¶]Division of Immunology, Allergy and Retrovirology; Department of Pediatrics, Texas Children's Hospital and Baylor College of Medicine, Houston, TX, USA.

[‖]Department of Molecular and Human Genetics; Human Genome Sequencing Center; Department of Pediatrics, Texas Children's Hospital and Baylor College of Medicine, Houston, TX, USA.

[#]Division of Hematology-Oncology; Department of Medicine, NCI Designated Cancer Center, University of Virginia, Charlottesville, VA, USA.

[**]Blood and Marrow Transplantation and Cell Therapy Program, Columbia University Irving Medical Center, New York, NY, USA.

[††]Department of Pathology and Cell Biology, Columbia University Irving Medical Center, New York, NY, USA.

Abstract

Natural killer (NK) cell deficiency (NKD) occurs when an individual's major clinical immunodeficiency derives from abnormal NK cells and is associated with several genetic etiologies. Three categories of β actin-related diseases with over 60 *ACTB* (β actin) variants have previously been identified, none with a distinct NK cell phenotype. An individual with mild developmental delay, macrothrombocytopenia, susceptibility to infections, molluscum, and EBV-associated lymphoma had functional NK cell deficiency for over a decade. A *de novo* *ACTB* variant encoding G342D β actin was identified and was consistent with the individual's developmental and platelet phenotype. This novel variant also was found to have direct impact in NK cells, as its expression in human NK YTS (YTS-NKD) cells caused increased cell spreading in lytic immune synapses created on activating surfaces. YTS-NKD cells were able to degranulate

Corresponding Author jso2121@cumc.columbia.edu.

and perform cytotoxicity, but demonstrated defective serial killing owing to prolonged conjugation to the killed target cell and thus were effectively unable to terminate lytic synapses. G342D β actin results in a novel mechanism of functional NKD via increased synaptic spreading and defective lytic synapse termination with resulting impaired serial killing leading to overall reductions in NK cell cytotoxicity.

Keywords

Natural killer cells; Inborn errors of immunity; Natural killer cell deficiency; Beta actin (ACTB); Cytotoxicity; Serial killing

Introduction

Inborn errors of immunity (IEI) are monogenic diseases caused by immune defects impacting one or more types of immune cells (1). There have been at least 485 IEI described to date. Natural killer cell deficiencies (NKD) are a type of IEI in which the major clinically relevant immunodeficiency results from abnormality of natural killer (NK) cells (2). NK cells are innate lymphocytes specialized for surveillance and elimination of virally infected or malignant cells and participate in inflammatory responses (3). NKDs are subdivided into classical (cNKD), those impacting the survival, proliferation, and/or development, limiting function, or functional (fNKD), solely impacting the cytotoxic function. Clinically, NKD presents as atypical susceptibility to or manifestations of viral infections, typically those of the herpesvirus or wart-causing virus families, along with increased malignancy risk (4). When patients present with possible NKD, broader IEI that includes an NK cell abnormality, such as NEMO or Wiskott Aldrich syndrome are also considered (5,6).

Beta actin (β/ ACTB), one of six highly conserved actin isoforms, is ubiquitously expressed in non-muscle cells with critical functions within the cytoskeleton (7). Globular actin (G-actin) is polymerized into filamentous actin (F-actin) and reversely depolymerized building F-actin networks through interactions with actin binding proteins (ABP) (8,9). These cytoskeletal proteins support cellular proliferation, migration, and cell-to-cell contact. Absence of β actin results in embryonic lethality in mouse models (10). Single nucleotide variants identified in patients have all been heterozygous and result in a clinical spectrum related to exonal position.

NK cell cytotoxicity is a stepwise mechanistic process of eliminating a triggering target cell through contact mediated degranulation of the contents of lysosomal organelles known as lytic granules (LG) (11). NK cells engage with a target cell and induce cytotoxicity based on overwhelming activating signals resulting from activating receptor ligation. This quickly triggers the formation of a specialized cell contact optimized for cytotoxicity called the lytic immune synapse (IS) (12). The lytic immune synapse is comprised of a highly organized cortical F-actin network that supports conjugation and enables the downstream processes required for killing (13). Lytic granules, specialized vesicles containing lytic components such as perforin and granzymes, are moved from throughout the cell to the microtubule-organizing center (MTOC) in a process called convergence, before polarizing to the lytic synapse (14). Once polarized, the lytic granules identify openings in a dynamic

synaptic cortical actin meshwork and are able to fuse with the NK cell membrane and degranulate (15,16). Thereafter, lytic components are secreted onto the target cell where they induce target cell death (17). The NK cell then begins downregulating activating receptors before terminating the IS and detaching from the deceased target cell (18). NK cells can go on to kill multiple target cells in this manner through a process called serial killing (19,20).

Normal actin function in NK cells has been described as essential to receptor engagement, IS formation, and lytic granule polarization. The specificity of β actin's role to these processes is unclear. In our work to better understand NKD, we have identified an individual with a β actin variant and impaired cytotoxicity that has identified specific roles for β actin in the cytolytic process.

Methods

Patient sample preparation

This study was reviewed by the Institutional Review Board at Children's Hospital of Philadelphia, Baylor College of Medicine, and Columbia University Irving Medicial Center and approved under protocols CHOP 2006–7-4885, BCM H-30487, and CUIMC AAAR7377. Blood samples were collected, following consent to these protocols, in sodium heparin collection tubes and peripheral blood mononuclear cells (PBMC) were isolated using a Ficoll-Paque Plus density gradient (45–001-750; GE Healthcare), in accordance with the guidelines established by the Declaration of Helsinki.

Sequencing

Exome sequencing was conducted and analyzed at Baylor College of Medicine according to the protocols previously established (21–23). Variants of significance were estalished through multiple biostatistical tests listed (24,25). Variants of interest as potential causative genes were selected for Sanger sequencing for confirmation.

Cell lines

K562 (CCL-243; ATCC), 721.221, and YTS cell lines were used from maintained laboratory stocks and regularly checked for mycoplasma by PCR testing. YTS-WT and -NKD lines were estalished from Lenti ORF clone ACTB-MYC-DKK tagged plasmid (RC203643L3; Origene). Cloning removed MYC-DKK, adding a c-terminus spacer and mScarlet fluorescent protein. The variant insertion for G342D β actin and all plasmid construction was done by Epoch Life Sciences, Inc. (Sugar Land, TX USA) (26). YTS-C, -WT, and -NKD cells were transduced with Lipofectamine 3000 following manufactuer's instructions (100022052; Invitrogen) and maintained according to protocols previously published with the addition of puromycin (A1113803; Gibco) for selection (27).

Flow cytometry

NK cells from PBMC samples were identified by antibodies Qdot 605 CD56 (HCD56; Biolegend) and Qdot 705 CD3 (SK7; Biolegend) and analyzed on LSR Fortessa (BD Biosciences) at Baylor College of Medicine. YTS cell lines were dyed/stained with Live/Dead Fixable Blue (L23105A; Invitrogen), BV605 CD56 (HCD56; 318334; Biolegend), and

BV785 CD3 (UCHT1; 300472; Biolegend). Cytofix/Cytoperm (554714; BD Biosciences) was used according to manufactuer's instructions and samples stained with Pacific Blue Granzyme B (GB11; 515407; Biolegend) and Alexa Fluor 488 Perforin (dG9; 308108; Biolegend).

For CD107a upregulation, YTS cells were incubated with 721.221 cells at 1:2 and PE-Cyanine5 CD107a (eBioH4A3; 15–1079-42; Invitrogen) for listed timepoints before fixation. All cell line studies were analyzed using the Biorad ZE5 Cell Analyzer (Bio-Rad Biosciences, Inc.) in the Columbia Stem Cell Initiative Flow Cytometry core facility at Columbia University Irving Medical Center and analyzed with Flowjo v.10.6.2 (BD Life Sciences).

Western blot

Lysates from YTS cell lines were prepared with Pierce RIPA Buffer (89901; Thermo Scientific) and HALT protease buffer (78430; Thermo Scientific) and run on Bolt Bis-Tris 4–12% 10 well gel (NW04120BOX; Thermo Scientific) in MOPS running buffer (B000102; Life Technologies). Protein was transferred onto nitrocellulose membrane 0.2 μm pore size (LC2000; Thermo Scientific) in Bolt transfer buffer (BT00061; Life Technologies). Antibodies used were: ACTB (4C2; MABT825; Millipore Sigma) and ACTG (2A3; MABT824; Millipore Sigma), 1:2000, and loading controls NM-2a (Poly19098; 909802; Biolegend) and β tubulin (E10; SC58880; Santa Cruz Biotechnologies), 1:5000. Secondary antibodies used were IRDye Goat anti-Mouse IgG (680RD; 926–68070; LI-COR Biosystems) and IRDye Goat anti-Rabbit IgG (800CW; 926–32211; LI-COR Biosystems). Blots were analyzed on the Li-Cor Odyssey CLx system alongside Odyssey one-color protein molecular weight marker (928–40000; LI-COR Biosystems).

Fixed cell imaging

All fixed cell imaging was performed using samples prepared in an 8 well chamber with #1.5 glass, fixed and permeabilized with Cytofix/cytoperm (554714; BD Biosciences) according to manufacturer's instructions, and imaged in 1x PBS (14–190-235; Fisher Scientific). Images were captured on Zeiss Axio Observer Z1 outfitted with a Yokogawa CSU-W1 T2 50 μm spinning disc and six lasers (405 nm, 445 nm, 488 nm, 505 nm, 561 nm, 637 nm). All images were captured using a 100x objective (NA= 1.46) and Prime 95B back illuminated sCMOS camera. Image analysis was performed with Imaris v8 (Oxford Instruments) or Fiji software (ImageJ) (28).

For actin spreading assays, chamber wells were coated with poly-L-lysine (PLL; P8920–100ML; Sigma Aldrich), 5 μg/mL of anti-CD18 (1B4/CD18; 373402; Biolegend) and/or anti-CD28 antibodies (CD28.2; 302933; Biolegend). Cells were added to the chamber wells in culture media and incubated at 37°C 5% CO_2 for 30 minutes. Cells were fixed and permeabilized with Cytofix/Cytoperm (554714; BD Biosciences) and stained with phalloidin (Alexa Fluor 405; A30104; Invitrogen). Images were analyzed in Fiji for area or mean fluorescent intensity (MFI) of individual cells. Single cells were confirmed by brightfield image and phalloidin signal was thresholded to limit background signal and

identify positive phalloidin signal. Thresholded phalloidin signal was used as the mask and all masked signal per individual cell was selected to be included in the calculation.

For fixed cell conjugation assays, YTS and 721.221 cells were mixed at a 2:1 ratio in 200 μL culture media and incubated for 25 minutes at 37°C 5% CO_2 before being placed in PLL coated chambers and incubated for another 20 minutes. Cells were fixed and permeabilized with Cytofix/Cytoperm (554714; BD Biosciences) and stained with phalloidin (Alexa Fluor 405; A30104; Invitrogen), perforin (Alexa Fluor 488, dG9; 308108; Biolegend), and α tubulin (Alexa Fluor 647, 10D8; 627908; Biolegend). Principles for measuring lytic granule (LG)-to-MTOC and MTOC-to-immune synapses (IS) were previously published and adjusted for Imaris analysis (29). Lytic granules and MTOC were detected at 0.5 μm and 1.0 μm threshold, respectively, using Imaris' spot filter. The IS was identified using the surface filter with a 1.0 μm threshold and isolated to cell-to-cell junctions.

Chromium-51 release functional assay

NK cell function of PBMC samples were assessed by 4-hour ^{51}Cr-release assay as described (6). PBMC and YTS cells were co-cultured with K562 and 721.221 target cells, respectively, for 4 hours in culture media at 37°C 5% CO_2. Serial killing was measured using lower effector to target ratios as described (19).

Live cell imaging

YTS cell lines were imaged with 721.221 cells to measure duration of conjugation, cytotoxicity, and new conjugate formation. YTS were labeled with Cell Tracker Red CMTPX (C34552; Invitrogen) and 721.221 with Calcein green (Alexa Fluor 488; C34852; Invitrogen)(1:500) and mixed 1:2. 721.221 cells were washed and added in 250 μL of culture media to a 24 well plate and incubated for 30 minutes at 37°C 5% CO_2. YTS cell lines were washed and gently added in 200 μL of culture media. Imaging was started immediately and continued every 2 minutes for 12 hours using the Incucyte S3 live-cell analysis system at 10x objective with 488 and 647 nm filter sets.

Images were assembled into stabilized stacks and manually analyzed in Fiji. Total conjugation time was calculated from the 12-hour end time of the assay or conjugation termination from initial contact between the YTS and 721.221 cells. Time for target cell death was measured from initial contact to total loss of Calcein green signal in the 721.221 cell. Time for new conjugate formation followed YTS cells and measured time from death of the previously conjugated target cell and initial contact with a new target cell.

Statistics and Graphics

Statistics were calculated using GraphPad Prism v.9.5.1 (GraphPad Software, San Diego, California USA). Outliers were removed using ROUT test with Q=1%. Normality was measured by Shapiro-Wilks test and determined the significance statistical tests listed. Graphics were developed using Biorender.com.

Data respository

Data files can be found at the following Dryad repository link: https://doi.org/10.5061/dryad.98sf7m0qz.

Results

Proband clinical presentation and history.

The male proband born to nonconsanguineous parents without relevant family history initially had failure to thrive, ophthalmoplegia (Duane syndrome- treated surgically), and macrothrombocytopenia. He had short stature, mild facial dysmorphisms, and mild developmental delay with normal brain MRI. Testing for MYH9-related disease was negative.

The proband experienced recurrent otitis media starting in the first year of life which required 3 tympanostomy tube placements. At age 3, he was hospitalized with RSV bronchiolitis, as well as pneumonia of unclear etiology on numerous occasions. At age 20, he presented with severe molluscum (MCV) (Fig. 1A), which persisted >1yr, but improved after 10mo cimetidine/topical steroids/topical antibiotics/biweekly destructive cryotherapy. This prompted immunodeficiency consideration. He had hypergammaglobulinemia with low IgM and PPV23 vaccination response (Table SI) and was treated with immunoglobulin replacement. Lymphocyte subsets were within normal ranges including NK cells and both mature $CD56^{dim}$ and immature $CD56^{bright}$ NK cell subsets (Table SI, Fig. 1B). Because of the severity of viral illness, additional evaluation of NK cells was advanced, finding detailed phenotypic testing was normal compared to our established ranges, suggesting normal maturation which has previously been shown to require intact migration (not shown) (30–32). Functional testing was performed using ^{51}Cr-release assay of PBMC with K562 target cells (Fig. 1C). Compared to a healthy donor and the mean of 205 healthy donors, the proband had significantly lower cytotoxic function (repeated over 3yr).

At age 30, the proband presented with fever, weight loss, and adenopathy. The proband initially underwent conventional therapy with ABVD (doxorubicin (Adriamycin), bleomycin, vinblastine, dacarbazine) x2 cycles with no complication. Interim PET/CT (Positron emission tomography–computed tomography) after cycle 2 showed decreased size and resolved fluorodeoxyglucose (FDG) avidity of multiple lymph nodes present, but increased FDG avidity from standard uptake value (SUV) 13.1 to SUV 22.8 of the left external iliac chain lymph node conglomerate. These findings were scored as 4 on the Deauville five-point scale, consistent with progressive disease.

Subsequently, the proband had multiple lymph node (LN) biopsies over a year of treatment from the groin and external iliac regions. All LN samples were involved by frank lymphomatous process with shared immunomorphological features. The biopsies showed complete effacement of LN architecture by variably sized aggregates and sheet-like infiltrates of large, atypical lymphocytes (Figure 1D, panels 1–3). This included a morphologic spectrum, ranging from centroblast-like cells to Hodgkin (H) and Reed-Sternberg (RS) cells, including H-RS variants and mummified cells. Small lymphocytes were seen admixed, which varied in density in different areas. Numerous histiocytes

and scattered plasma cells and eosinophils were noted. Variable coagulative necrosis and capsular thickening by fibrosis were also seen.

The neoplastic lymphocytes exhibited aberrant immunophenotype via immunohistochemical (IHC) staining by (Figure 1D, panels 4–7): $CD45^{+/-}$, $CD30^{+}$, $CD15^{+/-}$, Pax5 (Paired Box 5) $weak^{+}$, $CD20^{-}$, $CD79a^{-}$, $BCL6^{+/-}$ (B-cell lymphoma 6), $BCL2^{+/-}$ (B-cell lymphoma 2), $MUM1^{+}$ (multiple myeloma 1), and PD-$L1^{+}$ (programmed death ligand 1). The neoplastic cells were Epstein-Barr virus (EBV) positive by Epstein-Barr virus-encoded small RNAs in situ hybridization (EBER ISH)(Figure 1D, panel 8). The findings overall were indicative of extensive involvement by a primary immunodeficiency-associated lymphoproliferative disorder (IA-LPD), EBV^{+} lymphoma with Hodgkin-like features. IA-LPDs comprise a heterogeneous group of lesions with variable clinicopathologic features, which can share similar pathologic features (histology, immunophenotype, and genetic features) despite diverse clinical settings (33). Most typically, IA-LPDs are B-cell lymphoproliferative disorders (B-cell LPDs), usually EBV positive, showing a spectrum of lesions, including hyperplasias, polymorphic LPDs, and aggressive lymphomas.

The proband received treatment with rituximab (R) to address the EBV viremia also present and continued chemotherapy switching to escalated EPOCH (Etoposide phosphate, Prednisone, Vincristine sulfate (Oncovin), Cyclophosphamide, Doxorubicin hydrochloride (Hydroxydaunorubicin)). After 2 cycles of R-EPOCH, restaging PET/CT showed stable disease and the proband was enrolled on a phase 1b/2 clinical trial using the experimental oral HDAC inhibitor VRx-3996 & Valganciclovir in combination with valganciclovir in subjects with EBV-associated lymphoid malignancies at a different institution but discontinued the treatment due to progressive disease. Subsequently, the proband was then briefly treated with several lines of therapy, including rituximab in combination with brentuximab (an anti-CD30 antibody-drug conjugate), pembrolizumab (an anti-PD-1 antibody), and ibrutinib (a BTK inhibitor) without response. This was followed by treatment with three infusions of allogeneic EBV-specific cytotoxic T-lymphocytes (CTL), resulting in clinical improvement in constitutional symptoms and transfusion requirements, but mixed response on imaging studies. The proband succumbed to an episode of fungal pneumonia at age 31.

Identifying a novel β actin variant in fNKD proband.

Trio exome sequencing of the proband and biological parents was used to identify any genetic variants that may be affecting NK cell function. Although no known pathogenic alterations were identified, a number of candidate genetic variants were considered based upon their zygosity, heritability, prevalence in the population, and predicted damage to the gene (Supplemental Fig. 1A). Of these, a novel *de novo* variant c.G1025A p.G342D in β actin was most compelling. This variant results in a substitution of a glycine residue for an aspartic acid in the translated sequence affecting a highly conserved residue predicted to lie at the base of a critical structural pocket for protein binding and monomeric conformational changes (Supplemental Fig. 1 B,C) (34–37). Trio Sanger sequencing confirmed this variant in the proband as *de novo* (Fig. 1D). Variants in β actin result in a clinical spectrum with 3 distinct rare diseases already classified: Baraitser-Winter Syndrome 1 (BRWS1), *ACTB*-

associated syndromic thrombocytopenia (*ACTB*-AST), and Beta actin deficiency (BAD) (Table I). Few clinical cases of dystonia have been attributed to *ACTB* variants and are often diagnosed under BRWS1 (38–44). While most β actin variants were originally classified as causing BRWS1, few have been reclassified as *ACTB*-AST, causing thrombocytopenia and only moderate to mild cranio-facial malformations and developmental delay (42,45,46). In an emerging *ACTB* allelic series, BRWS1 and *ACTB*-AST are genetically distinct in that variant alleles associated with the former affects exons 1–4 and the latter exons 5 and 6. BAD is a longstanding, separate phenotype defined in a single proband having characteristics of *ACTB*-AST along with a neutrophil defect causing immunodeficiency not characteristic of either BRWS1 or *ACTB*-AST (47). Similar to BAD, our proband presents clinically with a phenotype similar to *ACTB*-AST with both variants G342D (NKD) and G364K (BAD) in exon 6 of β actin. Despite these similarities, our proband had an NK cell phenotype not identified in previously described β actin variants.

G342D β actin impairs NK cell cytotoxicity without affecting lytic granule convergence or polarization.

To evaluate if G342D β actin could cause an aberration of NK cell function, an immortalized human NK cell line, YTS, was used to study the variant in isolation from the proband's broader genetic and clinical context. YTS cells were transduced with lentivirus containing wildtype β actin (YTS-WT) or G342D β actin (YTS-NKD) and kept under puromycin selection so that stably expressing lines could be generated and tested against a YTS control cell line (YTS-C). The YTS-WT and -NKD cell lines demonstrated similar growth kinetics and were propagated equivalently *in vitro*, suggesting intact cell division and proliferation.

To determine any impact of the variant upon NK cell function, ^{51}Cr-release assay used with 721.221 target cells due to their susceptibility to YTS-mediated cytotoxicity (48). Across varying effector to target (E:T) ratios, YTS-NKD cells had significantly less specific lysis of target cells than YTS-C or YTS-WT (Fig. 2A). Expression of WT β actin did have some slight effect on the killing relative to YTS-C, but both were >4-fold higher when considering the number of YTS cells required to achieve a given percentage of target cell lysis than YTS-NKD cells. Thus, YTS-NKD cells expressing G342D β actin recapitulate the proband's functional NK cell defect, aligning with the criteria for single patient studies, and support further mechanistic investigation (49).

Overexpressing β actin in these cell lines had the potential to alter the expression of actin isoforms. The β actin isoform can influence cell motility, increasing it when overexpressed, unlike γ actin (10,50). Conversely, β actin knockdown decreases cell mobility and availability of globular actin (51). To evaluate the effect of G342D β actin expression on β and γ actin homeostasis, YTS cell lines were evaluated by Western blot. No significant relative difference of either β or γ isoforms were found in the transduced lines (YTS-WT and -NKD) compared to the YTS-C (Supplemental Fig. 2). The G342D β actin variant nor the expression of exogeneous WT β actin appeared to impact actin isoform homeostasis.

To evaluate the mechanism of cytotoxicity impaired by β actin G342D, the cytolytic machinery and its function was studied. The actin cytoskeleton, in addition to its cellular roles for mobility and development, is required for synapse formation and for polarization of

specialized vesicles, lytic granules (LG). The LG contain perforin and granzymes which are released onto the target cell during degranulation. Intracellular flow cytometric measurement of key lytic effectors demonstrated that both perforin and granzyme B were not decreased in YTS-NKD cells (Fig. 2B). Since the lytic effector molecules were present, and given the known roles of actin in establishing a lytic immunological synapse required for cytotoxicity, we next evaluated the cell biological stages of NK cell cytotoxicity. To determine if these processes were affected by the presence of G342D β actin, YTS cell lines were conjugated to 721.221 target cells to create lytic synapses, fixed, stained, and evaluated using fluorescence confocal microscopy. Projections through the z-axis demonstrated that LG convergence to the microtubule organizing center (MTOC) and LG polarization to the synapse were occurring (Fig. 2C). These were quantified in individual conjugates derived from multiple independent experiments. Measuring convergence as the mean distance of the LG from the MTOC in individual cells identified no difference between any of the cell lines (Fig. 2D, left). To measure polarization, the distance of the MTOC to the synapse was defined in individual cells which was not significantly different in YTS-NKD cells compared to the others (Fig. 2D, right). However, distance of MTOC to IS was decreased in YTS-WT compared to YTS-C. Overall, the internal movement of lytic machinery appeared intact in the presence of G342D in β actin.

One of the final actin dependent steps in positioning the lytic machinery is the secretion of the lytic granule contents onto the target cell. This process, degranulation, requires lytic granules to move through the F-actin of the lytic synapse. To evaluate whether degranulation was impaired by G342D β actin, CD107a upregulation was measured by flow cytometry. After co-incubation with 721.221 target cells, YTS-C, -WT and -NKD cells all demonstrated CD107a upregulation which increased with prolonged conjugation times (Fig. 2E). There were no significant differences in CD107a intensity between the cell lines at any given timepoint. Thus, the function of cytolytic machinery was not affected by the presence of the proband's β actin variant.

G342D β actin increases cell spreading and impairs serial killing.

While lytic granule polarization and degranulation were not altered by G342D β actin, there are other actin-related functions that enable synaptic function, some delineated by primary immunodeficiencies (15,16,52–54). To further evaluate synaptic actin, we studied cell spreading on glass visualizing F-actin, which we have previously shown governs optimal cytotoxicity (55). In order to simulate different types of synapses, we studied YTS cells on glass surfaces coated with poly-L-lysine (PLL) for a non-activating signal, anti-CD18 (β2 integrin) for an adhesion signal, anti-CD28 as triggering for degranulation, and anti-CD18 and -CD28 together (both adhesion and triggering). The CD28 receptor on YTS cells is the primary triggering receptor for cytotoxicity and is present on approximately 50% of mature human NK cells (31,48,56). Minimal spreading of cells was seen without stimulation on PLL (Fig. 3A). The engagement of CD18 gave rise to a larger F-actin footprint with some of the central hypodensity characteristic of a maturing synapse. This was accentuated further still with CD28 engagement or CD18/CD28. Some of the focal hypodensities in the synaptic actin, which we have shown allow for lytic granule passage, were also more clearly visible after CD28 engagement in YTS-C cells (15,57). When comparing the YTS-C cells (Fig. 3A,

top) to the same conditions for YTS-WT (Fig. 3A, middle) and YTS-NKD (Fig. 3A, bottom) cells, the general synaptic constructs did not appear different, but the synaptic interface appeared larger in cells containing G342D β actin. This observation suggests that the variant might have an impact on cell spreading as governed by F-actin structuring.

To quantify, synaptic actin per unit area of synapse, its mean fluorescence intensity (MFI) in individual cells across independent experiments was measured. The MFI of phalloidin was not significantly different across PLL, CD18, or CD28 conditions for YTS-C, -WT, or -NKD cell lines (Supplemental Fig. 3A). Interestingly, YTS-NKD cells stimulated via CD18/CD28 had significantly lower phalloidin MFI than YTS-C or -WT cells. This indicates less F-actin per unit area in these cells and suggests a more diffuse F-actin network. It should be noted that while not significantly different, there was a large spread of values and lower mean for the YTS-NKD cells activated via CD28 alone, suggesting the same indication as for CD18/CD28 stimulated cells.

Given the F-actin MFI and cell appearance, we wanted to measure the overall size of the synaptic interface as an indication of cell spreading. We quantified the total surface area of phalloidin signal, irrespective of intensity, using F-actin as an indicator of the synapse itself. YTS-C cells spread minimally on PLL or CD28 coated surfaces, which was increased with CD18 ligation (Fig. 3B, left) (15). Thus, adhesion signals promoted significant cell spreading as denoted by the size of the F-actin synaptic interface. The expression of WT β actin, however, led to increased cell spreading when CD28 was engaged by itself, in addition to the increased spreading induced by CD18. The YTS-NKD cells also demonstrated both CD18 and CD28-induced cell spreading like YTS-WT cells. The surface area of the synapse in YTS-NKD, however, was 20%, 41%, 37% and 42% larger than that found in the YTS-WT cells when comparing PLL, CD18, CD28 and CD18/28, respectively ($p<0.01$)(Supplemental Figure 3B). Thus, the G342D β actin variant increases synaptic surface area and promotes likely greater cell spreading across all conditions. With increased F-actin spreading, it is possible that YTS-NKD cells are not challenged in forming a synapse nor completing a single cytotoxic event, but perhaps are challenged in re-organizing F-actin after killing.

After the initial killing event, an NK cell terminates the synaptic connection and detaches from the dying or deceased target cell. It then has the potential to progress to kill a subsequent target cell, a process known as “serial killing”. To determine if serial killing capabilities were affected by the expression of G342D β actin, a variation on the 4-hour ^{51}Cr-release assay was performed to assess for serial killing (20). Specifically, very low ratios of YTS to target cells were used to allow each NK cell the opportunity to contact multiple targets to potentially engage in serial killing. Even in the presence of vast excesses of target cells, YTS-NKD cells were less effective than YTS-C or -WT cells (Fig. 4). Thus, even in a very target rich environment, despite being saturated with opportunities to kill multiple cells (while demonstrating normal cytotoxic mechanisms of convergence, polarization, and degranulation), fewer were killed by YTS-NKD cells. This suggests that G342D in β actin impairs an NK cell’s ability to kill multiple target cells via reduced serial killing.

G342D β actin increases synaptic conjugation time.

Given the increased cell spreading, decreased F-actin per unit area, and potentially reduced serial killing attributed to G342D β actin, we wanted to evaluate the later stages of lytic synapse, termination and detachment. To best visualize and measure the “end” of the synapse, we performed long-term live cell imaging of YTS cells incubated with 721.221 target cells (1:2 E:T ratio) at low resolution and low magnification. YTS cell lines were labeled with CellMask Red for identification, and 721.221 cells were labeled with Calcein green to allow them to be identified as well to determine when they have died via loss of the green fluorescence. Imaging was performed over 12 hours with images captured at 2-minute intervals. Time lapse video sequences of the cytolytic process were generated to evaluate individual conjugation events and representative images of YTS-WT and -NKD cells were selected (Fig. 5A). Sequences from a representative video (Supplementary Video 1) of a YTS-WT cell (red) killing a 721.221 target cell (green) identified initial conjugation in panel 2. Target cell membrane blebbing, an early indicator of cell death, was seen by panel 4. This was followed by the elimination of the Calcein green signal in panel 5 signifying target cell death and ultimately detachment of the YTS-WT from the deceased target in panel 6. At this point an NK cell would be capable of binding to a new target cell to engage in serial killing. Sequences from a representative video (Supplementary Video 2) of a YTS-NKD cell (red) killing a 721.221 target cell identified conjugation in panel 1. The conjugation persisted through target cell membrane blebbing and Calcein green signal loss in panel 3. In panels 4–6, the YTS-NKD cell moved positions, but failed to detach from the target cell prior to the end of the assay. Thus, the YTS-NKD cell demonstrated impaired synapse termination as detachment from the dead target cell did not occur. This would, in theory, limit the ability of this YTS-NKD cell to mediate subsequent kills.

To quantify the biology depicted by the representative images, multiple conjugates were evaluated across several experiments and the time of conjugate initiation to target cell detachment or end of the assay was measured. YTS-NKD cells had significantly longer conjugation times with 721.221 target cells on average than either YTS-C or YTS-WT cells (Fig. 5B, left). The time from initial conjugation to target cell Calcein release was also measured to determine the time required to mediate cell death. Despite longer total conjugation times in YTS-NKD cells, there was no significant difference in conjugate duration for target cell death when compared to YTS-C or -WT cells on average (Fig. 5B, center). The time for a given YTS cell to form a conjugate with a new 721.221 target cell after killing a previously conjugated target was also measured. YTS-C cells can form a new conjugate with target cells at an average of 213 minutes (Fig. 5B, right). While this increases in YTS-WT cells to an average of 303 minutes, it was significantly increased further still in YTS-NKD cells to an average of 409 minutes. Thus, the presence of the G342D β actin variant increases conjugation time and time to initiate a serial engagement. Thus, G342D β actin increases conjugation time and time to initiate a serial engagement, which we believe to be due to abnormal F-actin function, as evidenced by increased cell spreading. The resulting abnormality in NK cell function induced by G342 β actin, therefore occurs likely after the primary kill by preventing effective serial killing.

Discussion

We have studied an individual with recurrent infection, severe MCV, and an EBV-associated malignancy with longstanding functional NKD. They were found to have a G342D variant in β actin which we believe to be causative. Distinct from other β actin related disorders, the functional NK cell defect dominated the proband's clinical phenotype and aligns with those identified in other NKD cases (58,59). The previously identified spectrum of disorders associated with β actin variants have not been, with one exception, associated with immunodeficiency. Variants found in exons 1–4 cause BRWS1 which presents with distinct cranio-facial malformations and developmental delay (42). *ACTB*-AST presents with mild to moderate craniofacial malformations and developmental delay with macrothrombocytopenia. This seemingly less severe phenotype is associated with variants in exons 5 and 6. The molecular basis for *ACTB*-AST is impaired binding dynamics to other actin binding proteins (ABP) such as non-muscle myosin IIa (NM-IIa), filamin A, and α actinin (45). The single IEI related to *ACTB*, β actin deficiency, is caused by an E364K β actin variant, but was defined by a neutrophil defect associated with their migratory impairment. Our proband's clinical phenotype, despite extra-immune phenotypic overlap with *ACTB*-AST, was identified as a novel fNKD which we believe is a specific feature of the G342D β actin variant.

β actin deficiency and the case we describe are within the broader category of actin-related IEI referred to as actinopathies (60). Collectively, these have some common clinical presentations of recurring bacterial and/or viral infections, cutaneous lesions, and pulmonary infections (61). Some are also characterized by thrombocytopenia, which occurs with the WASp-related, *MYH9*-related, and *ARPC1B* syndromes, similar to our proband (62–66). Importantly, our proband had macrothrombocytopenia like individuals with MYH9-related disorders, which is distinct from the typical microthombocytopenia caused by *WASP* and *ARPC1B* variants. This speaks to potentially distinct pathophysiologies while still being actin-related. Of note, our proband did not present with an inflammatory phenotype associated with GTPase actinopathies such as *CDC42, RHOG, and RHOH* (67–69). Furthermore, variants in *ARPC1B*, *CORO1A*, *HEM1*, *WDR1*, *WASP* and *WIP* have all been associated with cell spreading abnormalities in their T cell immune synapses defining specific lymphocyte abnormalities and turning attention to activation-induced actin dynamics (70–76). Many have also been associated with defects in NK cell function (6,53,77,78). This combined with the identification of defects in our own proband led us to consider what the impact of the G342D variant in β actin was in the context of the many known actin-dependent processes in NK cells (13).

A functional and regulated cytoskeleton, including actin, has been established as essential for NK cell cytotoxicity. This network enables immune synapse formation, lytic granule polarization, and degranulation alongside other cellular functions. While these roles have not specifically been attributed to β actin in NK cells, they have been connected to the integrity of F-actin and many related binding proteins, such as WASP, WIP, and coronin-1A. More broadly, β actin is embryonic lethal when deleted from mouse genomes and functionally contributes to normal motility and developmental functions within cells (10). With the importance of actin in NK cell cytotoxic and cellular functions, we pursued variant G342D

β actin as causative for our proband's decreased NK cell cytotoxicity. On a cellular level, degranulation, which is also a more broadly actin-dependent function, occurred normally as evidenced via CD107a upregulation in the presence of G342D b actin across a range of conjugation times. Further, we identified increased synaptic surface area in YTS-NKD cells containing the G342D variant. This was specifically visualized in our actin spreading assay in which YTS-NKD cells demonstrated significantly larger F-actin footprints on activating surfaces as compared to their YTS-C or -WT counterparts. In consideration of the potential implications of this aberrant spreading, we functionally identified a serial killing defect in variant expressing cells. We observed in live cell imaging that target cells are rapidly and effectively killed, but that detachment from the dead target cell was delayed or even not observed. This resulted in YTS-NKD cells having prolonged conjugation with target cells and a decreased ability to detach from them. We hypothesize the more diffuse but larger cell spreading footprint observed when expressing β actin G342D leads to the inability to effectively depolymerize and deconstruct the IS to detach from the deceased target cell. Interestingly, protein modeling of β actin variant G342D, demonstrates the alteration of an invariant residue proximal to that binding the actin depolymerization factor, cofilin-1 (79). Thus, G342D b actin may affect actin remodeling and increases cell spreading at the IS leading to abnormal detachment and IS termination. To our knowledge, this constitutes the first NKD or IEI associated with an impaired termination phase of the lytic synapse.

Serial killing, the capability of NK cells to perform multiple cytotoxic events, has garnered interest as a therapeutic strategy for cancer treatment by exploiting NK cell cytotoxicity. The potential for multiple cytotoxic events varies amongst individual NK cells as well as across different target cells although the exact reasons are unclear (19). When serial killing, NK cells use, recycle, or reproduce their lytic machinery and receptors although the process has not been previously studied in YTS cells (20). In general, however, the potential for NK cell serial killing is bolstered by effective detachment from a target cell following a cytotoxic event (80). Preventing cytotoxicity in NK cells prolongs this conjugation, while the death of the target cell triggers the detachment (81). If the NK cell detachment is impaired, it remains activated with high levels of internal calcium and cytokine production, which can lead to inflammatory clinical phenotypes (18). The G342D variant in our proband does not impair killing mechanisms within the NK cell and the absence of an inflammatory phenotype in the proband suggest the NK cell signaling may be downregulated following successful target killing. Thus, G342D β actin appears to impair the internal mechanisms of detachment, likely through actin restructuring via depolymerization. With this prolonged conjugation, the potential for NK cell serial killing becomes dependent on both the NK cell and the conjugated deceased target cell, limiting the efficacy of NK cytotoxicity. This effectively results in an impairment of overall NK cell cytotoxic capacity and resulting host defense. While β actin G342D impact on synaptic actin characteristics provides a new insight, the specific mechanisms directing NK cell conjugate detachment remain an open area for future study.

Specific roles for monomeric b actin could be considered outside of the proposed impact of the G342D variant on increased F-actin spreading and synapse termination. These include scaffolding roles for b actin in the context of its known essential integration in the dynactin complex and participation in resulting dynein function (82,83). Since we found the dynein-

dependent process of lytic granule convergence to be normal in the presence of G342D b actin, this hypothesis is unlikely. Another consideration is for an impact of G342D b actin on ratios of β:γ actin since the maintenance of the monomeric actin pool is controlled by β actin and would ultimately be important for F-actin functions (51). Along these lines proportional increases of γ to β actin is associated with increased spreading, diffuse and disorganized β actin bundles, and higher expression of ABPs such as Arp2/3, WAVE2, and cofilin-1 (84). That said, the presence of variant G342D β actin in our experiments did not alter β to γ actin ratios, de-emphasizing this hypothesis. The cellular data from our experiments suggests initially normal but ultimately unrestrained cell spreading that hampers the active detachment process from a dead target cell.

Expressing variant G342D β actin in NK cells increases the spreading capacity on all surface types: neutral, adhesion, triggering, or adhesion and triggering. We hypothesized with normal convergence, polarization, and degranulation, an initial killing event may be unaffected by this variant, but instead the subsequent efficacy of cytotoxicity would be limited. In live cell imaging of YTS-NKD cells, variant expressing cells have prolonged conjugation to target cells despite normal time to perform cytotoxicity, killing the target cell. We attributed this to increased spreading and impaired detachment from the target cell. By prolonging the conjugation of a functional NK cell to a dead target cell, the potential for subsequent target cell killing is limited and total cytotoxic function of NK cells over time is decreased. We propose that *in vivo* this would result in NK cells unable to clear a population of diseased cells before its expansion beyond what typically NK cells might reasonably control. This could result in a reduced ability to handle viral infection while T cells are preparing their defense as well as a reduced ability to provide surveillance for malignant cells, ultimately giving susceptibility to early cancer development. These would explain the clinical susceptibilities identified in our proband. Importantly, further studies aimed at delineating the exact threshold at which target cells outpace NK cell serial killing capabilities would allow for a better understanding of optimal killing requirements. These could be useful in considering overall definitions of cytotoxic cell immunodeficiencies as well as standards needed to be achieved in optimizing cellular therapeutic approaches to cancer. The specific attributes of G342D β actin, however, define it as impairing particular NK cell functions without debilitating other major immune mechanisms. This combined with the proband's clinical presentation led us to consider this particular variant of b actin as a cause of fNKD thus expanding the spectrum of human genetic variants that have a majority clinical immunodeficiency impact upon NK cells.

Supplementary Material

Refer to Web version on PubMed Central for supplementary material.

Acknowledgements

We would like to thank the proband of this study and his family for their participation and contributions to this work. We also thank the physicians who cared for and treated the proband, including those who furthered this work. We thank the listed authors and their teams from the Human Genome Sequencing Center at Baylor College of Medicine. We thank Michael Kissner and the Columbia Stem Cell Institute for their facilities and knowledge. We also thank Dr. Luis Mateo Pedroza, Dr. Yu Li, and Shira Eisman for their supportive efforts.

Funding Statement

This work was supported by NIH R01AI120989, R01AI067946 and NYFIRST to JSO, and R01AI137073 to EMM.

Abbreviations

IEI	Inborn errors of immunity
ACTB	beta actin/ β actin
NK	natural killer
NKD	natural killer cell deficiency
cNKD	classical natural killer cell deficiency
fNKD	functional natural killer cell deficiency
IS	immune synapse
MTOC	microtubule organization center
LG	lytic granule
G-actin	globular actin
ABP	actin binding proteins
MCV	Molluscum contagiousum virus
ABVD	A – doxorubicin (Adriamycin) B – bleomycin. V – vinblastine. D – dacarbazine (DTIC)
PET/CT	Positron emission tomography–computed tomography
FDG	fluorodeoxyglucose
SUV	standard uptake value
LN	lymph node
IA-LPD	immunodeficiency-associated lymphoproliferative disorder
EPOCH	E= Etoposide phosphate, P= Prednisone, O= Vincristine sulfate (Oncovin), C= Cyclophosphamide, H= Doxorubicin hydrochloride (Hydroxydaunorubicin)
R-EPOCH	R= Rituximab, E= Etoposide phosphate, P= Prednisone, O= Vincristine sulfate (Oncovin), C= Cyclophosphamide, H= Doxorubicin hydrochloride
BRWS1	Baraitser Winter Syndrome 1
BAD	Beta actin deficiency
ACTB-AST- ACTB	associated syndromic thrombocytopenia

C	control
WT	wildtype
PLL	poly-L-lysine
E:T	effector to target ratio

References

1. Tangye SG, Al-Herz W, Bousfiha A, Cunningham-Rundles C, Franco JL, Holland SM, Klein C, Morio T, Oksenhendler E, Picard C, Puel A, Puck J, Seppänen MRJ, Somech R, Su HC, Sullivan KE, Torgerson TR, and Meyts I. 2022. Human inborn errors of immunity: 2022 update on the classification from the international union of immunological societies expert committee. J Clin Immunol. 42: 1473–1507. [PubMed: 35748970]
2. Orange JS 2013. Natural killer cell deficiency. J Allergy Clin Immunol. 132: 515–525. [PubMed: 23993353]
3. Mace EM 2023. Human natural killer cells: Form, function, and development. J Allergy Clin Immunol. 151: 371–385. [PubMed: 36195172]
4. Mace EM, and Orange JS 2019. Emerging insights into human health and nk cell biology from the study of nk cell deficiencies. Immunol Rev. 287: 202–225. [PubMed: 30565241]
5. Orange JS, Brodeur SR, Jain A, Bonilla FA, Schneider LC, Kretschmer R, Nurko S, Rasmussen WL, Köhler JR, Gellis SE, Ferguson BM, Strominger JL, Zonana J, Ramesh N, Ballas ZK, and Geha RS 2002. Deficient natural killer cell cytotoxicity in patients with ikk-gamma/nemo mutations. J Clin Invest. 109: 1501–1509. [PubMed: 12045264]
6. Orange JS, Ramesh N, Remold-O'Donnell E, Sasahara Y, Koopman L, Byrne M, Bonilla FA, Rosen FS, Geha RS, and Strominger JL 2002. Wiskott-aldrich syndrome protein is required for nk cell cytotoxicity and colocalizes with actin to nk cell-activating immunologic synapses. Proc Natl Acad Sci U S A. 99: 11351–11356. [PubMed: 12177428]
7. Dominguez R, and Holmes KC 2011. Actin structure and function. Annu Rev Biophys. 40: 169–186. [PubMed: 21314430]
8. Svitkina T. 2018. The actin cytoskeleton and actin-based motility. Cold Spring Harb Perspect Biol. 10.
9. Winder SJ, and Ayscough KR 2005. Actin-binding proteins. J Cell Sci. 118: 651–654. [PubMed: 15701920]
10. Bunnell TM, and Ervasti JM 2010. Delayed embryonic development and impaired cell growth and survival in actg1 null mice. Cytoskeleton (Hoboken). 67: 564–572. [PubMed: 20662086]
11. Mace EM, Dongre P, Hsu HT, Sinha P, James AM, Mann SS, Forbes LR, Watkin LB, and Orange JS 2014. Cell biological steps and checkpoints in accessing nk cell cytotoxicity. Immunol Cell Biol. 92: 245–255. [PubMed: 24445602]
12. Orange JS 2008. Formation and function of the lytic nk-cell immunological synapse. Nat Rev Immunol. 8: 713–725. [PubMed: 19172692]
13. Ben-Shmuel A, Sabag B, Biber G, and Barda-Saad M. 2021. The role of the cytoskeleton in regulating the natural killer cell immune response in health and disease: From signaling dynamics to function. Front Cell Dev Biol. 9: 609532.
14. Mentlik AN, Sanborn KB, Holzbaur EL, and Orange JS 2010. Rapid lytic granule convergence to the mtoc in natural killer cells is dependent on dynein but not cytolytic commitment. Mol Biol Cell. 21: 2241–2256. [PubMed: 20444980]
15. Carisey AF, Mace EM, Saeed MB, Davis DM, and Orange JS 2018. Nanoscale dynamism of actin enables secretory function in cytolytic cells. Curr Biol. 28: 489–502.e489. [PubMed: 29398219]
16. Rak GD, Mace EM, Banerjee PP, Svitkina T, and Orange JS 2011. Natural killer cell lytic granule secretion occurs through a pervasive actin network at the immune synapse. PLoS Biol. 9: e1001151.

17. Mace EM, Wu WW, Ho T, Mann SS, Hsu HT, and Orange JS 2012. Nk cell lytic granules are highly motile at the immunological synapse and require f-actin for post-degranulation persistence. J Immunol. 189: 4870–4880. [PubMed: 23066148]

18. Srpan K, Ambrose A, Karampatzakis A, Saeed M, Cartwright ANR, Guldevall K, De Matos G, Önfelt B, and Davis DM 2018. Shedding of cd16 disassembles the nk cell immune synapse and boosts serial engagement of target cells. J Cell Biol. 217: 3267–3283. [PubMed: 29967280]

19. Bhat R, and Watzl C. 2007. Serial killing of tumor cells by human natural killer cells--enhancement by therapeutic antibodies. PLoS One. 2: e326. [PubMed: 17389917]

20. Prager I, Liesche C, van Ooijen H, Urlaub D, Verron Q, Sandström N, Fasbender F, Claus M, Eils R, Beaudouin J, Önfelt B, and Watzl C. 2019. Nk cells switch from granzyme b to death receptor-mediated cytotoxicity during serial killing. J Exp Med. 216: 2113–2127. [PubMed: 31270246]

21. Lupski JR, Gonzaga-Jauregui C, Yang Y, Bainbridge MN, Jhangiani S, Buhay CJ, Kovar CL, Wang M, Hawes AC, Reid JG, Eng C, Muzny DM, and Gibbs RA 2013. Exome sequencing resolves apparent incidental findings and reveals further complexity of sh3tc2 variant alleles causing charcot-marie-tooth neuropathy. Genome Med. 5: 57. [PubMed: 23806086]

22. Stray-Pedersen A, Sorte HS, Samarakoon P, Gambin T, Chinn IK, Coban Akdemir ZH, Erichsen HC, Forbes LR, Gu S, Yuan B, Jhangiani SN, Muzny DM, Rødningen OK, Sheng Y, Nicholas SK, Noroski LM, Seeborg FO, Davis CM, Canter DL, Mace EM, Vece TJ, Allen CE, Abhyankar HA, Boone PM, Beck CR, Wiszniewski W, Fevang B, Aukrust P, Tjønnfjord GE, Gedde-Dahl T, Hjorth-Hansen H, Dybedal I, Nordøy I, Jørgensen SF, Abrahamsen TG, Øverland T, Bechensteen AG, Skogen V, Osnes LTN, Kulseth MA, Prescott TE, Rustad CF, Heimdal KR, Belmont JW, Rider NL, Chinen J, Cao TN, Smith EA, Caldirola MS, Bezrodnik L, Lugo Reyes SO, Espinosa Rosales FJ, Guerrero-Cursaru ND, Pedroza LA, Poli CM, Franco JL, Trujillo Vargas CM, Aldave Becerra JC, Wright N, Issekutz TB, Issekutz AC, Abbott J, Caldwell JW, Bayer DK, Chan AY, Aiuti A, Cancrini C, Holmberg E, West C, Burstedt M, Karaca E, Yesil G, Artac H, Bayram Y, Atik MM, Eldomery MK, Ehlayel MS, Jolles S, Flatø B, Bertuch AA, Hanson IC, Zhang VW, Wong LJ, Hu J, Walkiewicz M, Yang Y, Eng CM, Boerwinkle E, Gibbs RA, Shearer WT, Lyle R, Orange JS, and Lupski JR 2017. Primary immunodeficiency diseases: Genomic approaches delineate heterogeneous mendelian disorders. J Allergy Clin Immunol. 139: 232–245. [PubMed: 27577878]

23. Yang Y, Muzny DM, Reid JG, Bainbridge MN, Willis A, Ward PA, Braxton A, Beuten J, Xia F, Niu Z, Hardison M, Person R, Bekheirnia MR, Leduc MS, Kirby A, Pham P, Scull J, Wang M, Ding Y, Plon SE, Lupski JR, Beaudet AL, Gibbs RA, and Eng CM 2013. Clinical whole-exome sequencing for the diagnosis of mendelian disorders. N Engl J Med. 369: 1502–1511. [PubMed: 24088041]

24. Karczewski KJ, Francioli LC, Tiao G, Cummings BB, Alföldi J, Wang Q, Collins RL, Laricchia KM, Ganna A, Birnbaum DP, Gauthier LD, Brand H, Solomonson M, Watts NA, Rhodes D, Singer-Berk M, England EM, Seaby EG, Kosmicki JA, Walters RK, Tashman K, Farjoun Y, Banks E, Poterba T, Wang A, Seed C, Whiffin N, Chong JX, Samocha KE, Pierce-Hoffman E, Zappala Z, O'Donnell-Luria AH, Minikel EV, Weisburd B, Lek M, Ware JS, Vittal C, Armean IM, Bergelson L, Cibulskis K, Connolly KM, Covarrubias M, Donnelly S, Ferriera S, Gabriel S, Gentry J, Gupta N, Jeandet T, Kaplan D, Llanwarne C, Munshi R, Novod S, Petrillo N, Roazen D, Ruano-Rubio V, Saltzman A, Schleicher M, Soto J, Tibbetts K, Tolonen C, Wade G, Talkowski ME, Neale BM, Daly MJ, and MacArthur DG 2020. The mutational constraint spectrum quantified from variation in 141,456 humans. Nature. 581: 434–443. [PubMed: 32461654]

25. Kircher M, Witten DM, Jain P, O'Roak BJ, Cooper GM, and Shendure J. 2014. A general framework for estimating the relative pathogenicity of human genetic variants. Nat Genet. 46: 310–315. [PubMed: 24487276]

26. Bindels DS, Haarbosch L, van Weeren L, Postma M, Wiese KE, Mastop M, Aumonier S, Gotthard G, Royant A, Hink MA, and Gadella TW Jr. 2017. Mscarlet: A bright monomeric red fluorescent protein for cellular imaging. Nat Methods. 14: 53–56. [PubMed: 27869816]

27. Banerjee PP, Pandey R, Zheng R, Suhoski MM, Monaco-Shawver L, and Orange JS 2007. Cdc42-interacting protein-4 functionally links actin and microtubule networks at the cytolytic nk cell immunological synapse. J Exp Med. 204: 2305–2320. [PubMed: 17785506]

28. Schindelin J, Arganda-Carreras I, Frise E, Kaynig V, Longair M, Pietzsch T, Preibisch S, Rueden C, Saalfeld S, Schmid B, Tinevez JY, White DJ, Hartenstein V, Eliceiri K, Tomancak P, and Cardona A. 2012. Fiji: An open-source platform for biological-image analysis. Nat Methods. 9: 676–682. [PubMed: 22743772]
29. Hsu HT, Carisey AF, and Orange JS 2017. Measurement of lytic granule convergence after formation of an nk cell immunological synapse. Methods Mol Biol. 1584: 497–515. [PubMed: 28255722]
30. Angelo LS, Banerjee PP, Monaco-Shawver L, Rosen JB, Makedonas G, Forbes LR, Mace EM, and Orange JS 2015. Practical nk cell phenotyping and variability in healthy adults. Immunol Res. 62: 341–356. [PubMed: 26013798]
31. Mahapatra S, Mace EM, Minard CG, Forbes LR, Vargas-Hernandez A, Duryea TK, Makedonas G, Banerjee PP, Shearer WT, and Orange JS 2017. High-resolution phenotyping identifies nk cell subsets that distinguish healthy children from adults. PLoS One. 12: e0181134.
32. Lee BJ, and Mace EM 2017. Acquisition of cell migration defines nk cell differentiation from hematopoietic stem cell precursors. Mol Biol Cell. 28: 3573–3581. [PubMed: 29021341]
33. Natkunam Y, Gratzinger D, Chadburn A, Goodlad JR, Chan JKC, Said J, Jaffe ES, and de Jong D. 2018. Immunodeficiency-associated lymphoproliferative disorders: Time for reappraisal? Blood. 132: 1871–1878. [PubMed: 30082493]
34. Barrie KR, Carman PJ, and Dominguez R. Conformation of actin subunits at the barbed and pointed ends of f-actin with and without capping proteins. Cytoskeleton. n/a
35. Gao J, and Nakamura F. 2022. Actin-associated proteins and small molecules targeting the actin cytoskeleton. Int J Mol Sci. 23.
36. Pollard TD 2016. Actin and actin-binding proteins. Cold Spring Harbor Perspectives in Biology. 8.
37. von der Ecken J, Heissler SM, Pathan-Chhatbar S, Manstein DJ, and Raunser S. 2016. Cryo-em structure of a human cytoplasmic actomyosin complex at near-atomic resolution. Nature. 534: 724–728. [PubMed: 27324845]
38. Freitas JL, Vale TC, Barsottini OGP, and Pedroso JL 2020. Expanding the phenotype of dystonia-deafness syndrome caused by actb gene mutation. Mov Disord Clin Pract. 7: 86–87. [PubMed: 31970217]
39. Aiyar L, Stumbaugh T, Hirata GI, Chen B, Lau HL, and Wallerstein RJ 2019. Prenatal presentation in a patient with baraitser-winter cerebrofrontofacial syndrome and a novel actb variant. Clinical Dysmorphology. 28: 162–164.
40. Cianci P, Fazio G, Casagranda S, Spinelli M, Rizzari C, Cazzaniga G, and Selicorni A. 2017. Acute myeloid leukemia in baraitser–winter cerebrofrontofacial syndrome. American Journal of Medical Genetics Part A. 173: 546–549. [PubMed: 27868373]
41. Sandestig A, Green A, Jonasson J, Vogt H, Wahlström J, Pepler A, Ellnebo K, Biskup S, and Stefanova M. 2019. Could dissimilar phenotypic effects of actb missense mutations reflect the actin conformational change? Two novel mutations and literature review. Mol Syndromol. 9: 259–265. [PubMed: 30733661]
42. Verloes A, Di Donato N, Masliah-Planchon J, Jongmans M, Abdul-Raman OA, Albrecht B, Allanson J, Brunner H, Bertola D, Chassaing N, David A, Devriendt K, Eftekhari P, Drouin-Garraud V, Faravelli F, Faivre L, Giuliano F, Guion Almeida L, Juncos J, Kempers M, Eker HK, Lacombe D, Lin A, Mancini G, Melis D, Lourenço CM, Siu VM, Morin G, Nezarati M, Nowaczyk MJ, Ramer JC, Osimani S, Philip N, Pierpont ME, Procaccio V, Roseli ZS, Rossi M, Rusu C, Sznajer Y, Templin L, Uliana V, Klaus M, Van Bon B, Van Ravenswaaij C, Wainer B, Fry AE, Rump A, Hoischen A, Drunat S, Rivière JB, Dobyns WB, and Pilz DT 2015. Baraitser-winter cerebrofrontofacial syndrome: Delineation of the spectrum in 42 cases. Eur J Hum Genet. 23: 292–301. [PubMed: 25052316]
43. Yates TM, Turner CL, Firth HV, Berg J, and Pilz DT 2017. Baraitser–winter cerebrofrontofacial syndrome. Clinical Genetics. 92: 3–9. [PubMed: 27625340]
44. Drury S, Williams H, Trump N, Boustred C, GOSGene N. Lench, Scott RH, and Chitty LS 2015. Exome sequencing for prenatal diagnosis of fetuses with sonographic abnormalities. Prenatal Diagnosis. 35: 1010–1017. [PubMed: 26275891]

45. Latham SL, Ehmke N, Reinke PYA, Taft MH, Eicke D, Reindl T, Stenzel W, Lyons MJ, Friez MJ, Lee JA, Hecker R, Frühwald MC, Becker K, Neuhann TM, Horn D, Schrock E, Niehaus I, Sarnow K, Grützmann K, Gawehn L, Klink B, Rump A, Chaponnier C, Figueiredo C, Knöfler R, Manstein DJ, and Di Donato N. 2018. Variants in exons 5 and 6 of actb cause syndromic thrombocytopenia. Nat Commun. 9: 4250. [PubMed: 30315159]
46. Greve JN, Schwäbe FV, Pokrant T, Faix J, Di Donato N, Taft MH, and Manstein DJ 2022. Frameshift mutation s368fs in the gene encoding cytoskeletal β-actin leads to actb-associated syndromic thrombocytopenia by impairing actin dynamics. Eur J Cell Biol. 101: 151216.
47. Nunoi H, Yamazaki T, Tsuchiya H, Kato S, Malech HL, Matsuda I, and Kanegasaki S. 1999. A heterozygous mutation of beta-actin associated with neutrophil dysfunction and recurrent infection. Proc Natl Acad Sci U S A. 96: 8693–8698. [PubMed: 10411937]
48. Gunesch JT, Angelo LS, Mahapatra S, Deering RP, Kowalko JE, Sleiman P, Tobias JW, Monaco-Shawver L, Orange JS, and Mace EM 2019. Genome-wide analyses and functional profiling of human nk cell lines. Mol Immunol. 115: 64–75. [PubMed: 30054012]
49. Casanova JL, Conley ME, Seligman SJ, Abel L, and Notarangelo LD 2014. Guidelines for genetic studies in single patients: Lessons from primary immunodeficiencies. J Exp Med. 211: 2137–2149. [PubMed: 25311508]
50. Peckham M, Miller G, Wells C, Zicha D, and Dunn GA 2001. Specific changes to the mechanism of cell locomotion induced by overexpression of beta-actin. J Cell Sci. 114: 1367–1377. [PubMed: 11257002]
51. Bunnell TM, Burbach BJ, Shimizu Y, and Ervasti JM 2011. B-actin specifically controls cell growth, migration, and the g-actin pool. Mol Biol Cell. 22: 4047–4058. [PubMed: 21900491]
52. Mizesko MC, Banerjee PP, Monaco-Shawver L, Mace EM, Bernal WE, Sawalle-Belohradsky J, Belohradsky BH, Heinz V, Freeman AF, Sullivan KE, Holland SM, Torgerson TR, Al-Herz W, Chou J, Hanson IC, Albert MH, Geha RS, Renner ED, and Orange JS 2013. Defective actin accumulation impairs human natural killer cell function in patients with dedicator of cytokinesis 8 deficiency. J Allergy Clin Immunol. 131: 840–848. [PubMed: 23380217]
53. Mace EM, and Orange JS 2014. Lytic immune synapse function requires filamentous actin deconstruction by coronin 1a. Proc Natl Acad Sci U S A. 111: 6708–6713. [PubMed: 24760828]
54. Orange JS, Roy-Ghanta S, Mace EM, Maru S, Rak GD, Sanborn KB, Fasth A, Saltzman R, Paisley A, Monaco-Shawver L, Banerjee PP, and Pandey R. 2011. Il-2 induces a wave2-dependent pathway for actin reorganization that enables wasp-independent human nk cell function. J Clin Invest. 121: 1535–1548. [PubMed: 21383498]
55. Gwalani LA, and Orange JS 2018. Single degranulations in nk cells can mediate target cell killing. J Immunol. 200: 3231–3243. [PubMed: 29592963]
56. Teng JM, Liu XR, Mills GB, and Dupont B. 1996. Cd28-mediated cytotoxicity by the human leukemic nk cell line yt involves tyrosine phosphorylation, activation of phosphatidylinositol 3-kinase, and protein kinase c. J Immunol. 156: 3222–3232. [PubMed: 8617944]
57. Sanborn KB, Rak GD, Mentlik AN, Banerjee PP, and Orange JS 2010. Analysis of the nk cell immunological synapse. Methods Mol Biol. 612: 127–148. [PubMed: 20033638]
58. Moon WY, and Powis SJ 2019. Does natural killer cell deficiency (nkd) increase the risk of cancer? Nkd may increase the risk of some virus induced cancer. Front Immunol. 10: 1703. [PubMed: 31379882]
59. Orange JS 2020. How i manage natural killer cell deficiency. J Clin Immunol. 40: 13–23. [PubMed: 31754930]
60. Kamnev A, Lacouture C, Fusaro M, and Dupré L. 2021. Molecular tuning of actin dynamics in leukocyte migration as revealed by immune-related actinopathies. Front Immunol. 12: 750537.
61. Dupré L, Boztug K, and Pfajfer L. 2021. Actin dynamics at the t cell synapse as revealed by immune-related actinopathies. Front Cell Dev Biol. 9: 665519.
62. Derry JM, Ochs HD, and Francke U. 1994. Isolation of a novel gene mutated in wiskott-aldrich syndrome. Cell. 78: 635–644. [PubMed: 8069912]
63. Kahr WH, Pluthero FG, Elkadri A, Warner N, Drobac M, Chen CH, Lo RW, Li L, Li R, Li Q, Thoeni C, Pan J, Leung G, Lara-Corrales I, Murchie R, Cutz E, Laxer RM, Upton J, Roifman CM, Yeung RS, Brumell JH, and Muise AM 2017. Loss of the arp2/3 complex component arpc1b

causes platelet abnormalities and predisposes to inflammatory disease. Nat Commun. 8: 14816. [PubMed: 28368018]

64. Kuijpers TW, Tool ATJ, van der Bijl I, de Boer M, van Houdt M, de Cuyper IM, Roos D, van Alphen F, van Leeuwen K, Cambridge EL, Arends MJ, Dougan G, Clare S, Ramirez-Solis R, Pals ST, Adams DJ, Meijer AB, and van den Berg TK 2017. Combined immunodeficiency with severe inflammation and allergy caused by arpc1b deficiency. J Allergy Clin Immunol. 140: 273–277.e210. [PubMed: 27965109]
65. Seri M, Pecci A, Di Bari F, Cusano R, Savino M, Panza E, Nigro A, Noris P, Gangarossa S, Rocca B, Gresele P, Bizzaro N, Malatesta P, Koivisto PA, Longo I, Musso R, Pecoraro C, Iolascon A, Magrini U, Rodriguez Soriano J, Renieri A, Ghiggeri GM, Ravazzolo R, Balduini CL, and Savoia A. 2003. Myh9-related disease: May-hegglin anomaly, sebastian syndrome, fechtner syndrome, and epstein syndrome are not distinct entities but represent a variable expression of a single illness. Medicine (Baltimore). 82: 203–215. [PubMed: 12792306]
66. Somech R, Lev A, Lee YN, Simon AJ, Barel O, Schiby G, Avivi C, Barshack I, Rhodes M, Yin J, Wang M, Yang Y, Rhodes J, Marcus N, Garty BZ, Stein J, Amariglio N, Rechavi G, Wiest DL, and Zhang Y. 2017. Disruption of thrombocyte and t lymphocyte development by a mutation in arpc1b. J Immunol. 199: 4036–4045. [PubMed: 29127144]
67. Kalinichenko A, Perinetti Casoni G, Dupré L, Trotta L, Huemer J, Galgano D, German Y, Haladik B, Pazmandi J, Thian M, Yüce Petronczki Ö, Chiang SC, Taskinen M, Hekkala A, Kauppila S, Lindgren O, Tapiainen T, Kraakman MJ, Vettenranta K, Lomakin AJ, Saarela J, Seppänen MRJ, Bryceson YT, and Boztug K. 2021. Rhog deficiency abrogates cytotoxicity of human lymphocytes and causes hemophagocytic lymphohistiocytosis. Blood. 137: 2033–2045. [PubMed: 33513601]
68. Lam MT, Coppola S, Krumbach OHF, Prencipe G, Insalaco A, Cifaldi C, Brigida I, Zara E, Scala S, Di Cesare S, Martinelli S, Di Rocco M, Pascarella A, Niceta M, Pantaleoni F, Ciolfi A, Netter P, Carisey AF, Diehl M, Akbarzadeh M, Conti F, Merli P, Pastore A, Levi Mortera S, Camerini S, Farina L, Buchholzer M, Pannone L, Cao TN, Coban-Akdemir ZH, Jhangiani SN, Muzny DM, Gibbs RA, Basso-Ricci L, Chiriaco M, Dvorsky R, Putignani L, Carsetti R, Janning P, Stray-Pedersen A, Erichsen HC, Horne A, Bryceson YT, Torralba-Raga L, Ramme K, Rosti V, Bracaglia C, Messia V, Palma P, Finocchi A, Locatelli F, Chinn IK, Lupski JR, Mace EM, Cancrini C, Aiuti A, Ahmadian MR, Orange JS, De Benedetti F, and Tartaglia M. 2019. A novel disorder involving dyshematopoiesis, inflammation, and hlh due to aberrant cdc42 function. J Exp Med. 216: 2778–2799. [PubMed: 31601675]
69. Szczawinska-Poplonyk A, Ploski R, Bernatowska E, and Pac M. 2020. A novel cdc42 mutation in an 11-year old child manifesting as syndromic immunodeficiency, autoinflammation, hemophagocytic lymphohistiocytosis, and malignancy: A case report. Front Immunol. 11: 318. [PubMed: 32231661]
70. Brigida I, Zoccolillo M, Cicalese MP, Pfajfer L, Barzaghi F, Scala S, Oleaga-Quintas C, Álvarez-Álvarez JA, Sereni L, Giannelli S, Sartirana C, Dionisio F, Pavesi L, Benavides-Nieto M, Basso-Ricci L, Capasso P, Mazzi B, Rosain J, Marcus N, Lee YN, Somech R, Degano M, Raiola G, Caorsi R, Picco P, Moncada Velez M, Khourieh J, Arias AA, Bousfiha A, Issekutz T, Issekutz A, Boisson B, Dobbs K, Villa A, Lombardo A, Neven B, Moshous D, Casanova JL, Franco JL, Notarangelo LD, Scielzo C, Volpi S, Dupré L, Bustamante J, Gattorno M, and Aiuti A. 2018. T-cell defects in patients with arpc1b germline mutations account for combined immunodeficiency. Blood. 132: 2362–2374. [PubMed: 30254128]
71. Mugnier B, Nal B, Verthuy C, Boyer C, Lam D, Chasson L, Nieoullon V, Chazal G, Guo XJ, He HT, Rueff-Juy D, Alcover A, and Ferrier P. 2008. Coronin-1a links cytoskeleton dynamics to tcr alpha beta-induced cell signaling. PLoS One. 3: e3467. [PubMed: 18941544]
72. Nolz JC, Medeiros RB, Mitchell JS, Zhu P, Freedman BD, Shimizu Y, and Billadeau DD 2007. Wave2 regulates high-affinity integrin binding by recruiting vinculin and talin to the immunological synapse. Mol Cell Biol. 27: 5986–6000. [PubMed: 17591693]
73. Salzer E, Zoghi S, Kiss MG, Kage F, Rashkova C, Stahnke S, Haimel M, Platzer R, Caldera M, Ardy RC, Hoeger B, Block J, Medgyesi D, Sin C, Shahkarami S, Kain R, Ziaee V, Hammerl P, Bock C, Menche J, Dupré L, Huppa JB, Sixt M, Lomakin A, Rottner K, Binder CJ, Stradal TEB, Rezaei N, and Boztug K. 2020. The cytoskeletal regulator hem1 governs b cell development and prevents autoimmunity. Sci Immunol. 5.

74. Sims TN, Soos TJ, Xenias HS, Dubin-Thaler B, Hofman JM, Waite JC, Cameron TO, Thomas VK, Varma R, Wiggins CH, Sheetz MP, Littman DR, and Dustin ML 2007. Opposing effects of pkctheta and wasp on symmetry breaking and relocation of the immunological synapse. Cell. 129: 773–785. [PubMed: 17512410]

75. Pfajfer L, Mair NK, Jiménez-Heredia R, Genel F, Gulez N, Ardeniz Ö, Hoeger B, Bal SK, Madritsch C, Kalinichenko A, Chandra Ardy R, Gerçeker B, Rey-Barroso J, Ijspeert H, Tangye SG, Simonitsch-Klupp I, Huppa JB, van der Burg M, Dupré L, and Boztug K. 2018. Mutations affecting the actin regulator wd repeat-containing protein 1 lead to aberrant lymphoid immunity. J Allergy Clin Immunol. 142: 1589–1604.e1511. [PubMed: 29751004]

76. Pfajfer L, Seidel MG, Houmadi R, Rey-Barroso J, Hirschmugl T, Salzer E, Antón IM, Urban C, Schwinger W, Boztug K, and Dupré L. 2017. Wip deficiency severely affects human lymphocyte architecture during migration and synapse assembly. Blood. 130: 1949–1953. [PubMed: 28903942]

77. Cook SA, Comrie WA, Poli MC, Similuk M, Oler AJ, Faruqi AJ, Kuhns DB, Yang S, Vargas-Hernández A, Carisey AF, Fournier B, Anderson DE, Price S, Smelkinson M, Abou Chahla W, Forbes LR, Mace EM, Cao TN, Coban-Akdemir ZH, Jhangiani SN, Muzny DM, Gibbs RA, Lupski JR, Orange JS, Cuvelier GDE, Al Hassani M, Al Kaabi N, Al Yafei Z, Jyonouchi S, Raje N, Caldwell JW, Huang Y, Burkhardt JK, Latour S, Chen B, ElGhazali G, Rao VK, Chinn IK, and Lenardo MJ 2020. Hem1 deficiency disrupts mtorc2 and f-actin control in inherited immunodysregulatory disease. Science. 369: 202–207. [PubMed: 32647003]

78. Volpi S, Cicalese MP, Tuijnenburg P, Tool ATJ, Cuadrado E, Abu-Halaweh M, Ahanchian H, Alzyoud R, Akdemir ZC, Barzaghi F, Blank A, Boisson B, Bottino C, Brigida I, Caorsi R, Casanova JL, Chiesa S, Chinn IK, Dückers G, Enders A, Erichsen HC, Forbes LR, Gambin T, Gattorno M, Karimiani EG, Giliani S, Gold MS, Jacobsen EM, Jansen MH, King JR, Laxer RM, Lupski JR, Mace E, Marcenaro S, Maroofian R, Meijer AB, Niehues T, Notarangelo LD, Orange J, Pannicke U, Pearson C, Picco P, Quinn PJ, Schulz A, Seeborg F, Stray-Pedersen A, Tawamie H, van Leeuwen EMM, Aiuti A, Yeung R, Schwarz K, and Kuijpers TW 2019. A combined immunodeficiency with severe infections, inflammation, and allergy caused by arpc1b deficiency. J Allergy Clin Immunol. 143: 2296–2299. [PubMed: 30771411]

79. Huehn AR, Bibeau JP, Schramm AC, Cao W, De La Cruz EM, and Sindelar CV 2020. Structures of cofilin-induced structural changes reveal local and asymmetric perturbations of actin filaments. Proc Natl Acad Sci U S A. 117: 1478–1484. [PubMed: 31900364]

80. Netter P, Anft M, and Watzl C. 2017. Termination of the activating nk cell immunological synapse is an active and regulated process. J Immunol. 199: 2528–2535. [PubMed: 28835459]

81. Anft M, Netter P, Urlaub D, Prager I, Schaffner S, and Watzl C. 2020. Nk cell detachment from target cells is regulated by successful cytotoxicity and influences cytokine production. Cell Mol Immunol. 17: 347–355. [PubMed: 31471588]

82. Lau CK, O'Reilly FJ, Santhanam B, Lacey SE, Rappsilber J, and Carter AP 2021. Cryo-em reveals the complex architecture of dynactin's shoulder region and pointed end. The EMBO Journal. 40: e106164.

83. Urnavicius L, Zhang K, Diamant AG, Motz C, Schlager MA, Yu M, Patel NA, Robinson CV, and Carter AP 2015. The structure of the dynactin complex and its interaction with dynein. Science. 347: 1441–1446. [PubMed: 25814576]

84. Dugina V, Khromova N, Rybko V, Blizniukov O, Shagieva G, Chaponnier C, Kopnin B, and Kopnin P. 2015. Tumor promotion by γ and suppression by β non-muscle actin isoforms. Oncotarget. 6: 14556–14571. [PubMed: 26008973]

Key Points

1. Variant G342D in β actin causes novel functional NK cell deficiency in our proband.
2. Variant expression increases spreading area when cytotoxicity is activated.
3. NK cell serial killing is delayed by prolonged conjugate interaction.

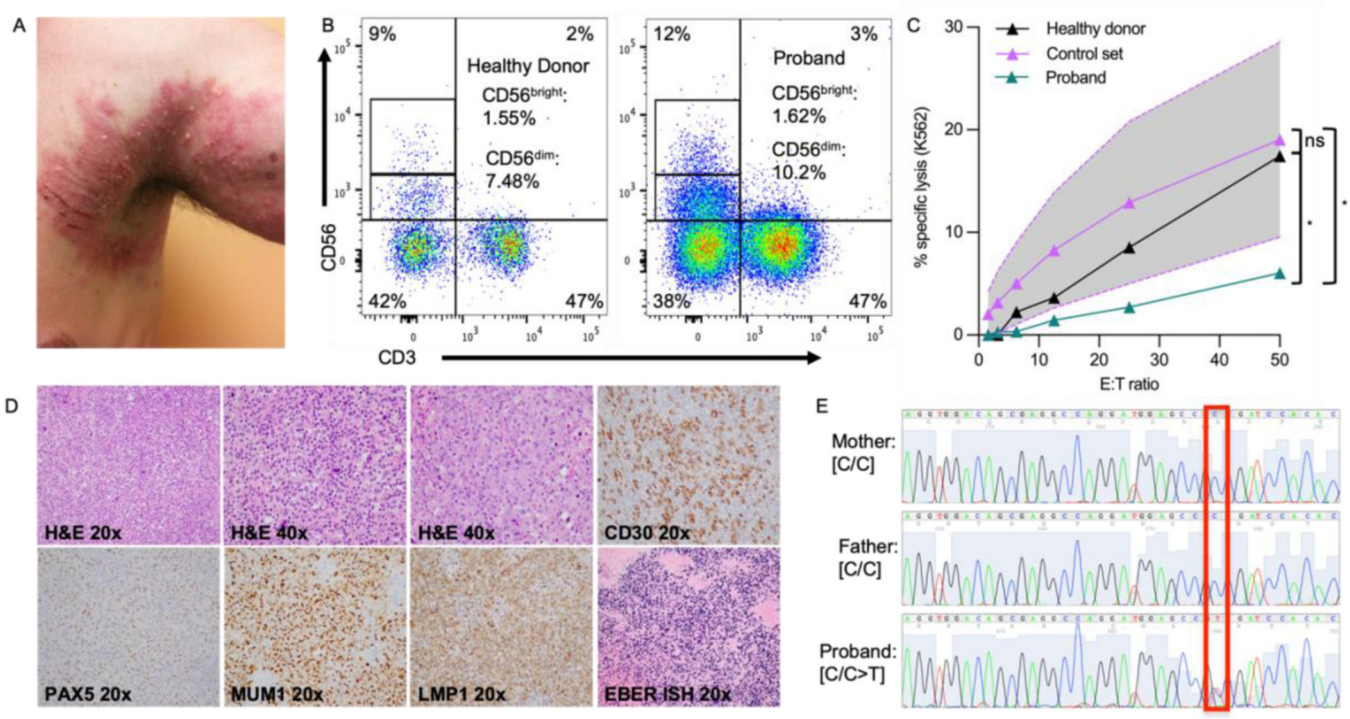

Figure 1: fNKD in association with a G342D ACTB variant.

(A) The proband had numerous viral infections including severe Molluscum contagiosum virus (MCV) at age 20. (B) PBMCs from a healthy donor and proband at age 24 evaluated for NK cells within a lymphocyte gate as $CD3^{-}CD56^{+}$ cells with gated regions specifying $CD56^{bright}$ and $CD56^{dim}$ populations. (C) NK cell cytotoxicity measured by ^{51}Cr-release assay using K562 target cells showing mean ± SD for healthy control donors (purple line, gray region n=205) and a lab control (black) and the proband (teal) at age 27 in which the proband is different via by Shapiro-Wilk test and paired ratio *t* test (NS, not significant, *P<0.05). (D) Immunohistochemical staining of lymph node biopsy samples defining primary immunodeficiency-associated lymphoproliferative disorder (IA-LPD), EBV^{+} lymphoma with Hodgkin-like features malignancy (individual stains and magnifications are listed and the H&E 20 and 40X show different magnifications of the same field). (E) Exome sequencing identified a c.G1025A *ACTB* alteration corresponding to a p.G342D in β actin confirmed as *de novo* in the proband via Sanger sequencing.

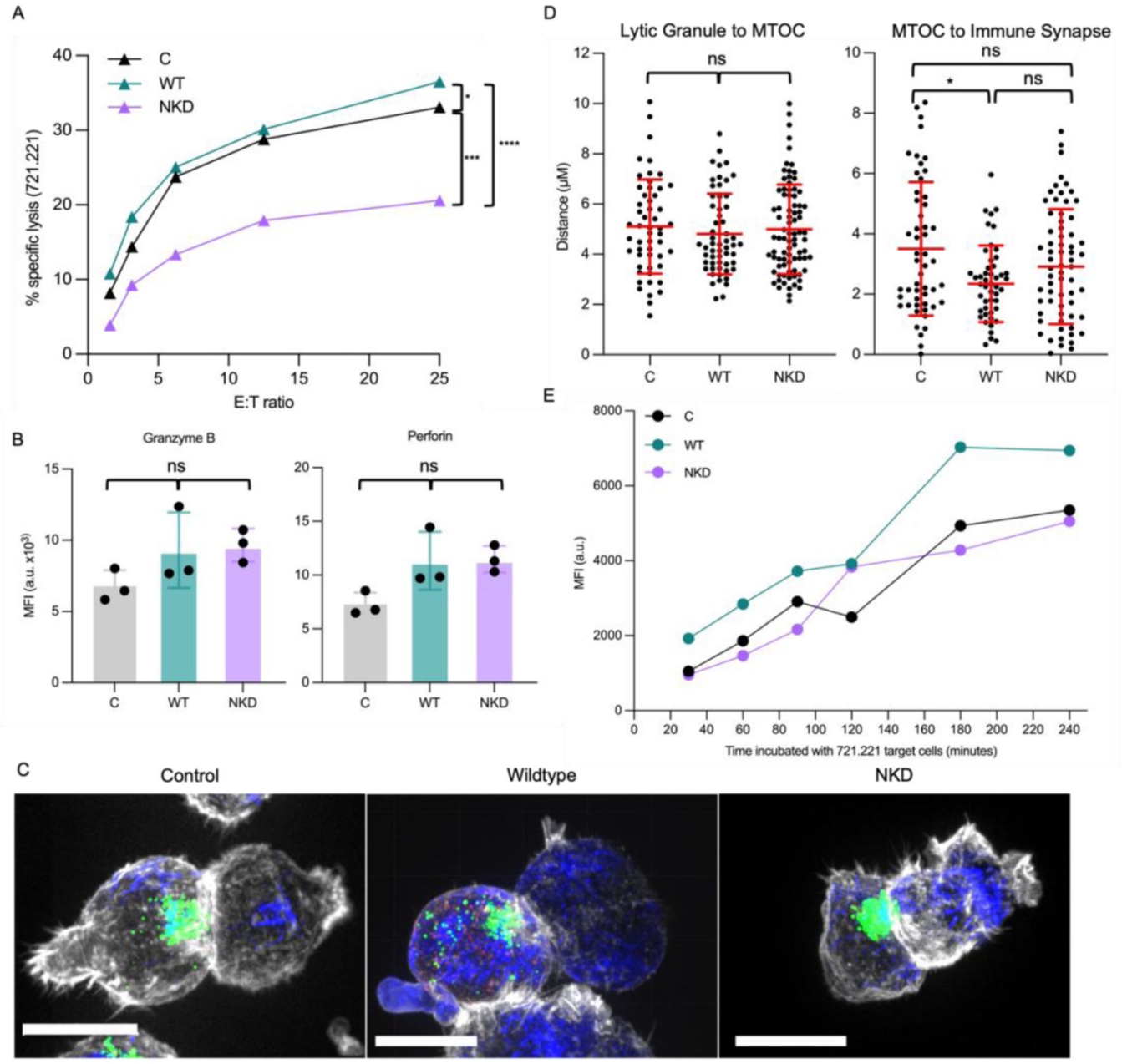

Figure 2: G342D ACTB variant impact in NK cells.

(A) Representative ^{51}Cr-release assay measuring specific lysis of 721.221 target cells by YTS control (C, black), WT β actin expressing (WT, teal), and G342D β actin expressing (NKD, purple) cells (Shapiro-Wilk test and paired ratio *t* test). (B) Flow cytometry mean fluorescent intensity (MFI) of mature perforin and granzyme B in YTS-C, -WT, and -NKD cell lines (Mann Whitney U test, mean of 3 independent experiments). (C) Representative images of fixed cell conjugates between 721.221 target cells and YTS-C, -WT, and -NKD (left to right) cells imaged after 45 minutes in conjugation, fixed, and stained for perforin (lytic granules, green), α-tubulin (MTOC and microtubules, blue), phalloidin (F-actin, white). Scale bar=15 μm. (D) Distance of lytic granules from the MTOC (defined by

tubulin density) measuring convergence and distance of MTOC to IS measuring polarization (Shapiro-Wilk test and Mann Whitney U test; outliers via ROUT test with Q= 1%, mean of 4 independent experiments with N=53–83 cells per condition). (E) CD107a MFI determined by flow cytometry of YTS cell lines in conjugation with 721.221 target cells across times from 30–240 minutes. Gates determined with YTS only control to exclude unconjugated cells and YTS selected by $CD3^{-}CD56^{+}$ cells. Across two independent experiments, YTS-NKD showed no difference in CD107a expression from YTS-C or -WT at any timepoint. (NS, not significant, *P<0.05, ***P<0.001, ****P<0.0001)

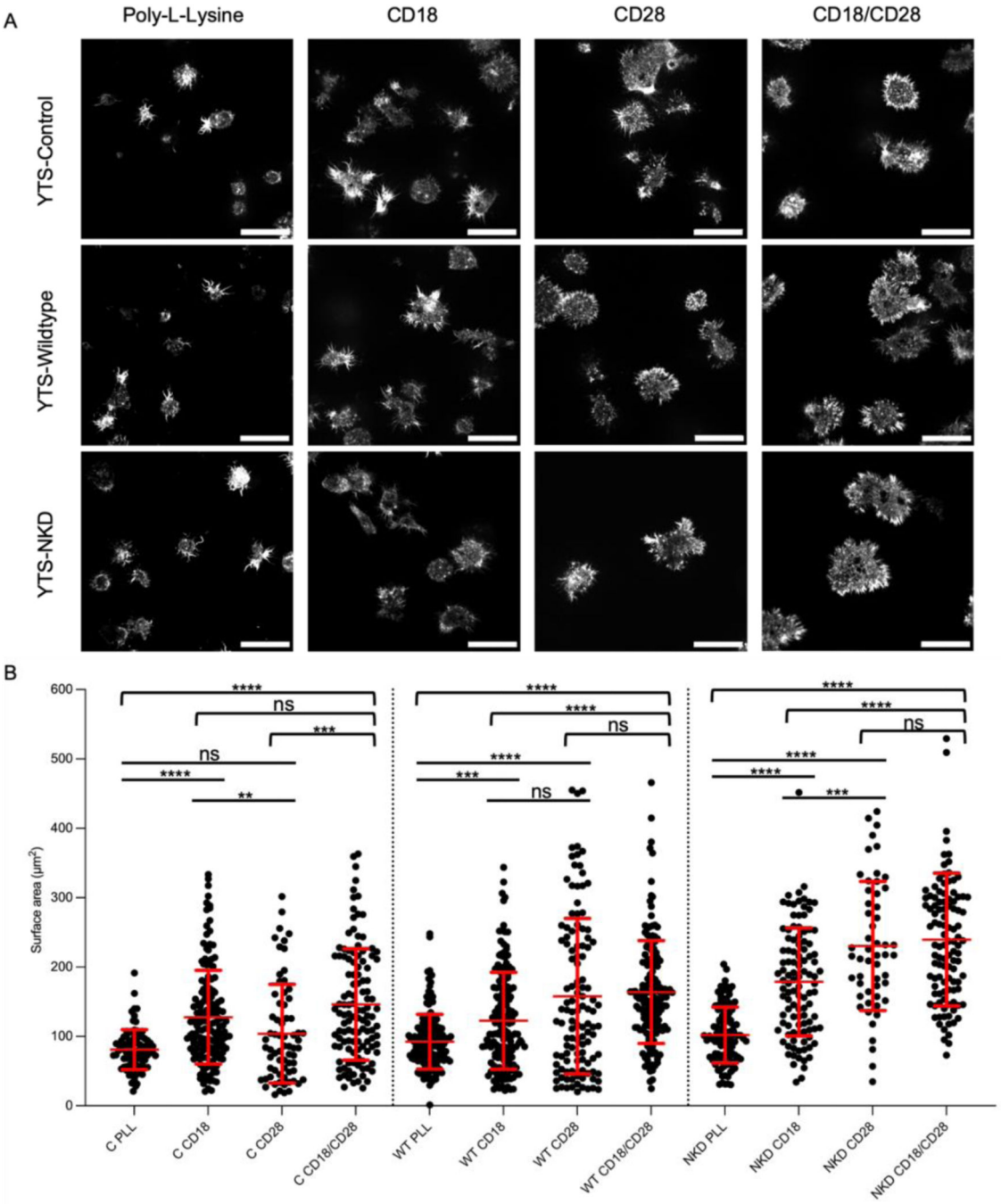

Figure 3: G342D ACTB expressing NK cells demonstrate increased activation-induced spreading.

(A) Representative images of YTS-C, -WT, and -NKD cells (top to bottom) incubated on poly-L-lysine (PLL), CD18, CD28, and CD18/CD28 coated slides (left to right) and stained with phalloidin (white) to bind F-actin and viewed at the plane of the glass. Scale bar=25 μm. (B) Comparison of cell surface area (μm^2) across cell lines and activation conditions measured by the masked area of phalloidin signal at the plane of the glass. N=72–332 cells per condition obtained over 3 independent experiments. Outliers were determined by ROUT test with Q= 1% and normality by Shapiro-Wilk test. Statistical significance was

determined by Mann-Whitney U test. (NS=not significant, *P<0.05, **P<0.01, ***P<0.001, ****P<0.0001)

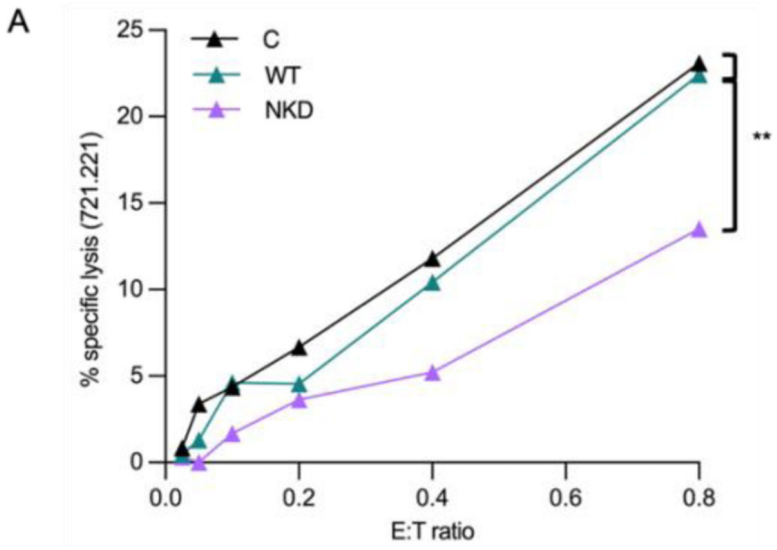

Figure 4: Impaired serial killing in G342D variant expressing NK cells.

Low E:T ratios were used in 4-hour ^{51}Cr-release assay to increase the number of 721.221 target cells available for each YTS-C (black), -WT (teal), or -NKD (purple) cell in order to evaluate serial killing ability. Points represent the means of technical triplicates from a representative experiment that was independently repeated 3 times. Specific lysis was tested by Shapiro-Wilk test and paired ratio *t* test. (**P<0.005)

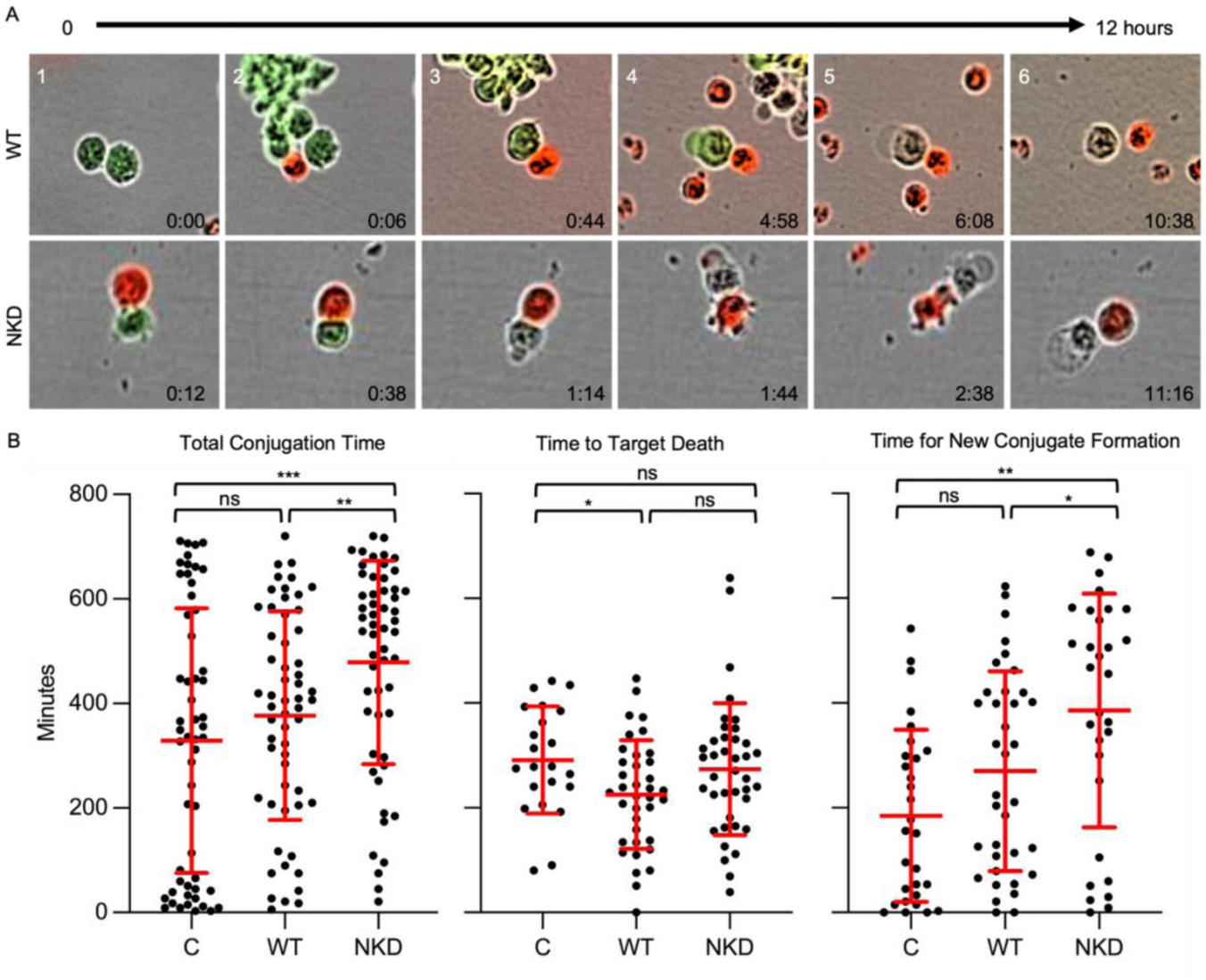

Figure 5: G342D variant expressing NK cells ineffectively terminate lytic synapses.

(A) Live cell fluorescent time lapse image sequence YTS-WT (top) and -NKD (bottom) cells (red) incubated with Calcein green-labelled 721.221 cells for 12 hours (time, black). Cell death can be visualized by calcein dye loss. In the WT sequence, conjugation begins in panel 2, death in panel 5 and detachment in panel 6. In the NKD sequence conjugation is seen in panel 1, death in panel 5 but detachment does not occur. (B) Measurement of total conjugate time (left), time to target cell death (middle) and time for a new conjugate to form (right) in 49–56 independent control (C), WT or NKD YTS cells with 721.221 target cells in 12h live cell imaging sequences. Outliers were determined by ROUT test with Q= 1% and normality by Shapiro-Wilk test. Statistical significance was determined by Mann-Whitney U test. (NS=not significant, *P<0.05, **P<0.01, ***P<0.001)

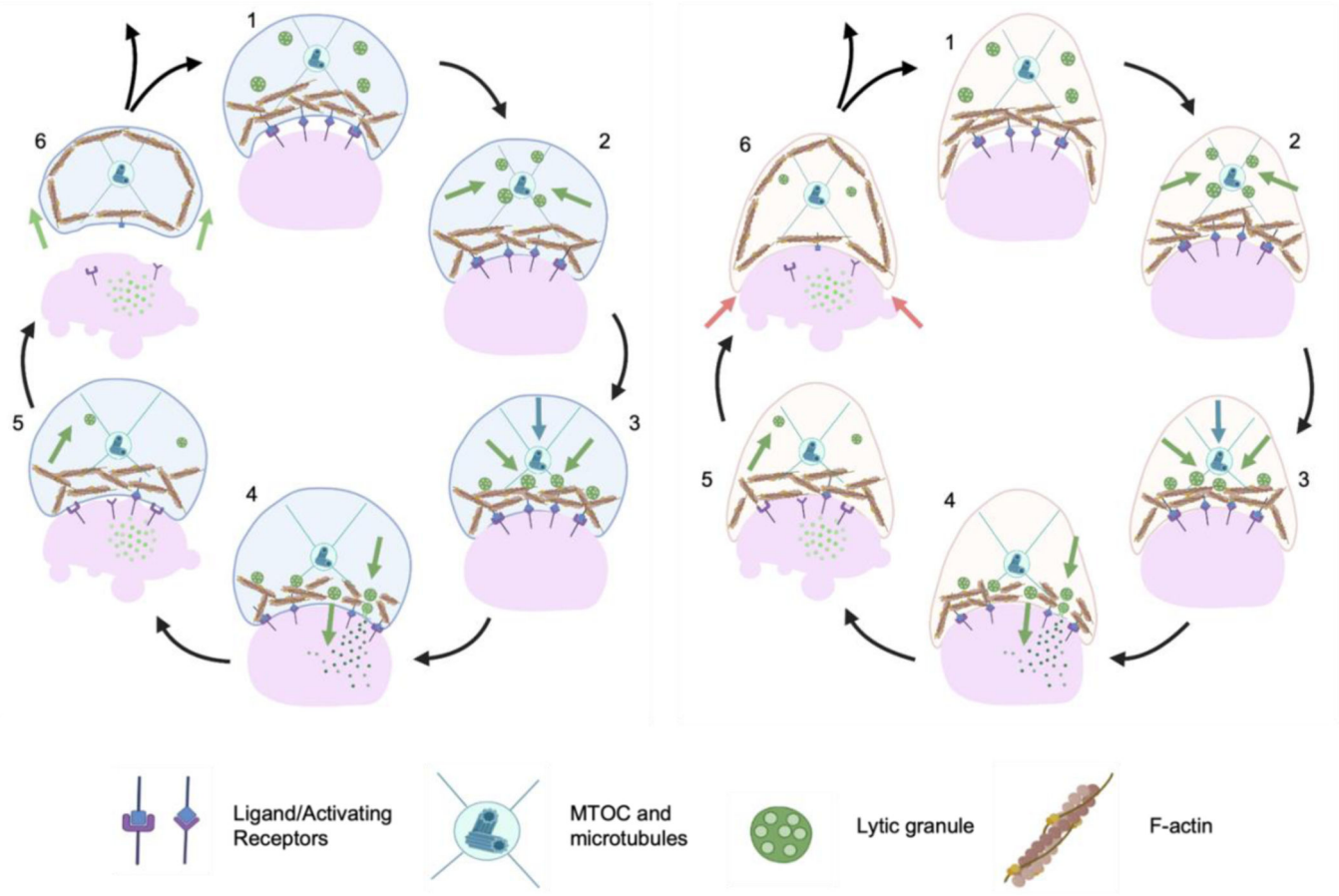

Figure 6: Model for G342D β actin impact upon NK cell cytotoxicity: impairment of serial killing.

Steps in normal NK cell cytotoxicity (left) or as proposed for the impact of G342D β actin (right). (1) An NK cell (top cell) requires contact-mediated ligation and activation upon receptor engagement with a target cell (bottom) to form a lytic immune synapse in the NK cell, which induces actin reorganization and convergence of lytic granules to the MTOC (2). Together, the lytic granules and MTOC polarize to the synapse (3) and identify conduits in the synaptic actin network for degranulation and release their contents onto the target cell (4). The target cell is then killed (5) after which a detachment event typically occurs (6) to allow for serial killing and a repeat of the cycle. In the context of G342D β actin (right), the NK cell spreads over the target cell to a greater extent (2–5) and is less able to detach (6) and becomes a less effective serial killer.

Table I:

Disorders and phenotypes associated with *ACTB* variants.

Disease	Variant(s)	Approximate # of Cases	Immunologic defects	Clinical Phenotype	Reference
Baraitser Winter Syndrome I (BRWS1)	Primarily variants in exons 1–4	39	Individual cases with malignancy development or repeat infections	Craniofacial dysmorphisms, microcephaly, moderate to severe developmental delay	(39–44)
ACTB-associated syndromic thrombocytopenia (*ACTB*-AST)	Variants in exons 5–6	7	Leukocytosis with increased eosinophil counts	Macrothrombocytopenia, mild craniofacial abnormalities, microcephaly, mild developmental delay	(44,45)
Beta actin deficiency (BAD)	E364K	1	Decreased neutrophil motility	Thrombocytopenia, developmental delay, impaired leukocyte migration	(44,46)
Functional natural killer cell deficiency (NKD)	G342D	1	Decreased NK cell cytotoxicity with normal NK cell frequency and phenotype	Atypical viral infections, macrothrombocytopenia, mild developmental delay, specific antibody deficiency, Hodgkin's lymphoma	This investigation

ACTB variants and associated disease classifications. Exon 1–4 variants: Baraitser-Winter Syndrome 1; exons 5–6 *ACTB*-associated syndromic thrombocytopenia (*ACTB*-AST); ACTB E364K, β-actin deficiency (BAD); and proband's NKD attributed to ACTB G342D.